Computational Biology and Chemistry 53 (2014) 184–190

Contents lists available at ScienceDirect

Computational Biology and Chemistry

journal homepage: www.elsevier.com/locate/compbiolchem

Molecular simulation investigation on the interaction between barrier-to-autointegration factor dimer or its Gly25Glu mutant and LEM domain of emerin

Yu-Dong Shang, Ji-Long Zhang, Yan Wang, Hong-Xing Zhang, Qing-Chuan Zheng *

State Key Laboratory of Theoretical and Computational Chemistry, Institute of Theoretical Chemistry, Jilin University, Changchun, Jilin 130023, PR China

ARTICLE INFO

Article history:
Received 21 May 2014
Received in revised form 17 September 2014
Accepted 19 September 2014
Available online 7 November 2014

Keywords:
Barrier-to-autointegration factor dimer (BAF2)
Molecular dynamics
Emerin
LEM domain
Point mutation

ABSTRACT

The interaction between barrier-to-autointegration factor dimer (BAF2) and LEM domain of emerin (Em^{LEM}) was studied by molecular simulation methods. Nonspecific fragment of double-strand DNA molecule was docked with each chain of BAF2 by ZDOCK program. The model of DNA2:BAF2:Em^{LEM} was thus constructed. The mutant Gly25Glu of BAF2 was manually constructed to explore the detailed effect of the mutation on the binding of BAF2 and Em^{LEM}. It has been experimentally suggested that point mutation Gly25Glu can disturb the binding between BAF2 and Em^{LEM}. Then, molecular dynamics (MD) simulations were performed on DNA2:BAF2(WT):Em^{LEM} and DNA2:BAF2(MT):Em^{LEM} complexes. 30 ns trajectories revealed that the trajectory fluctuations of MT complex are more violent than that of the WT complex. Further, the binding free energy analysis showed that the electronegative residues Asp57, Glu61 and Asp65 from chain A, glu36 from chain B of BAF2 mainly contribute to interact with Em^{LEM}. Besides, a stable $\pi-\pi$ stack between trp62 and phe39 from BAF2(WT) chain B is destroyed by Glu25 in BAF2(MT). As a result, trp62 forms an interaction with glu25, and phe39 converts to strengthen affinity to Em^{LEM}. On the other hand, Trp62 from chain A also forms a strong interaction with MT Glu25. Thus, with the docking of DNA, BAF2(MT) has higher affinity with Em^{LEM} than BAF2(WT).

1. Introduction

Emerin is a multiple domain lamina-associated polypeptide emerin-MAN1 (LEM) protein comprising an N-terminal globular LEM domain (Em^{LEM}), which is separated by a hydrophobic nuclear localization signal, and a C-terminal transmembrane region (Lin et al., 2000; Wolff et al., 2001). The structure of Em^{LEM} has two α-helices (residues 9–19 and 28–46). The α-helices form an angle for about 43° (Cai et al., 2007). Emerin localizes in the inner nuclear membrane (INM) of somatic mammalian cells, and requires A-type lamins (lamin A) (Haque et al., 2010; Wheeler and Ellis, 2010; Zhang et al., 2005; D'Angelo and Hetzer, 2006). Emerin regulates extracellular signal-regulated kinase (ERK) signaling (Muchir et al., 2007a,b, 2009) and directly binds transcription factors in developing myoblasts (Markiewicz et al., 2006; Tilgner et al., 2009; Holaska, 2008). Besides, genetic analysis yields important insights into their somatic roles (Huber et al., 2009). Human emerin and lamins mutations cause many diseases, including one or more tissues muscular dystrophy, bone, fat, connective tissue, skin, heart, blood or nervous, brain development and accelerate aging (Wolff et al., 2001; Liang et al., 2011).

Barrier-to-autointegration factor (BAF) is a small (10 kDa) double strand DNA (dsDNA)-binding protein, which is highly conserved among metazoans (Lee and Craigie, 1998). One molecule of Em^{LEM} binds a BAF dimer (BAF2) (Furukawa, 1999; Cai et al., 2001). BAF2 is necessary for assembly of emerin at the nuclear envelope (Capanni et al., 2012; Haraguchi et al., 2001). Additional roles for BAF2 in nuclear structure are suggested by its direct binding to nuclear lamins (Gruenbaum et al., 2005; Holaska et al., 2003). Interactions between BAF2 and LEM proteins at the 'core' region of telophase chromosomes are required to assemble lamin A filaments (Shimi et al., 2004; Segura-Totten and Wilson, 2004). BAF-null *Drosophila* cells fail to express cyclins, suggesting that BAF affects the gene expression of cyclin directly or indirectly (Furukawa et al., 2003). Excess BAF influences higher-order chromatin organization and nuclear envelope assembly (Segura-Totten et al., 2002).

The solution NMR structure of the BAF2:Em^{LEM} complex reveals that the binding surfaces on both BAF2 and Em^{LEM} consist of a central hydrophobic portion surrounded by a rim of polar and

* Corresponding author. Tel.: +86 431 88498966; fax: +86 431 88498966.
E-mail address: zhengqc@jlu.edu.cn (Q.-C. Zheng).

http://dx.doi.org/10.1016/j.compbiolchem.2014.09.007
1476-9271/

charged residues, which is typical in many protein:protein complexes (Williams et al., 2004). In human cells, expression of BAF missense mutation Gly25Glu dominantly disrupts the assembly of emerin, LAP2β and lamin A into reforming nuclei (Haraguchi et al., 2001). The Gly25 locates in the interface between BAF and DNA. Related experiment suggested that Gly25Glu mutation affected emerin localization during telophase. This BAF mutant is inactive for binding to DNA, and inactive for binding to emerin and LAP2 in vitro (Haraguchi et al., 2001). Our previous study (Shang et al., 2014) shows that Gly25Glu mutation can attenuate the interactions between BAF and DNA, which is consistent with experimental observation. We utilize molecular docking, point mutation and molecular dynamic (MD) simulation to compare the differences of structure and function between wild type (WT) BAF2:Em^{LEM} complex and Gly25Glu mutant type (MT) in BAF2:Em^{LEM} complex.

2. Theoretical methods

2.1. Docking study

ZDOCK module (Wiehe et al., 2005) of Discovery Studio 2.5 was used to perform the docking simulation of DNA with BAF. The structures of BAF2:Em^{LEM} complex and double strands DNA (dsDNA) were taken from Protein Data Bank (chain A in PDB code: 2ODG and chain B and C in 2BZF, respectively). The CHARMm Polar H force field (Grosdidier et al., 2011) was applied to depict all the atoms except non-polar H in molecular docking. 2000 top poses were generated and then classified into 60 clusters. The cutoff value of root-mean-square deviation (RMSD) was 1.0 Å, and interface cutoff was 2.0 Å (Accelrys Software Inc., 2007). Zrank scoring algorithm was then tested on ZDOCK benchmark dataset version 2.5 (Wiehe et al., 2005). Based on the related experimental result (Haraguchi et al., 2001), 'Build and edit proteins' module of Discovery Studio 2.5 (Accelrys Software Inc., 2007) was used to mutate Gly25 to Glu25 in BAF.

2.2. Molecular dynamics simulation

All the MD simulations were performed on Inspur workstations using the Amber11 software package (Case et al., 2005). The ff03ua force field (Ode et al., 2007) was used for energy minimization and MD simulations. The charge of DNA2:BAF2(WT):Em^{LEM} and DNA2:BAF2(MT):Em^{LEM} complexes were neutralized by tleap module of Amber11. An explicit solvent model TIP3P water box (Jorgensen et al., 1983) was used with a distance of 10.0 Å between complex surface and water box boundary. A minimization of 1000-step steepest descent (SD) and 1000-step conjugate gradient (CG) was carried out. The constraint force constant on protein was 500 kcal mol^{-1} Å^{-2}. After that, without any restraint on the whole system, a minimization of 3000-step SD and 4000-step CG was used. Then, a heating simulation was performed from 0 to 300 K in 500 ps with a weak constraint force constant value of 10.0 kcal mol^{-1} Å^{-2}. After heating, a NPT ensemble of 1 atm and 300 K was applied for 30 ns equilibrium simulation without any constraint. Periodic boundary condition was used to the system to obtain consistent behavior. The cutoff value of nonbonded interaction was 12.0 Å. The particle mesh Ewald (PME) method (Essmann et al., 1995) was employed for the computation of long-range electrostatic forces. The time step was 1.0 fs. A simple leapfrog integrator was used to propagate the dynamics, with the collision frequency of 1.0 ps^{-1}. A Langevin thermostat was adopted. The relaxation time for barostat bath was 2.0 ps. VMD (Humphrey et al., 1996) software was used to visualize the trajectories and to depict structural representations.

2.3. The calculations of binding free energy

The MM-GB/SA method implemented in Amber11 (Gohlke et al., 2003) was applied to calculate the binding free energy between the ligand and the receptor (Swanson et al., 2004). The binding free energy (ΔG_{bind}) in MM-GB/SA between a ligand (Em^{LEM}) and a receptor (BAF2) to form BAF2:Em^{LEM} complex was calculated as:

$$\Delta G_{bind} = G_{complex} - G_{receptor} - G_{ligand} \quad (1)$$

$$G = E_{MM} + G_{sol} - TS \quad (2)$$

$$E_{MM} = E_{int} + E_{ele} + E_{vdw} \quad (3)$$

$$G_{sol} = G_{GB} + G_{SA} \quad (4)$$

In Eq. (2), the E_{MM},G_{sol}, and TS represented molecular mechanics component in gas phase, the stabilization energy due to solvation, and a vibrational entropy term, respectively. E_{MM} was given as a sum of E_{int}, E_{ele}, and E_{vdw} which were internal, Coulomb and van der Waals interaction terms, respectively. Solvation energy, G_{sol}, was separated into an electrostatic solvation free energy (G_{GB}) and a nonpolar solvation free energy (G_{SA}). The former could be obtained from the generalized born (GB) method. The latter was considered to be proportional to the molecular solvent accessible surface area (SASA) (Hou et al., 2008). The binding free energies were obtained by averaging over the values calculated for 2000 snapshots from the 11–20 ns of the trajectories at 5 ps intervals for the complex structures.

2.4. Determination of π–π stacking interaction

We adopted the following tests to determine stacked and staggered π–π interactions (McGaughey et al., 1998; Wen et al., 2012): the default center distance cutoff was set to 8.0 Å to define the distance between the centroid of each pair of aromatic rings. For these, an atom from each ring should be within the closest atom distance cutoff (4.5 Å); the angle θ between the normal of one ring and the centroid–centroid vector must fall between 0° and ±the θ angle cutoff (default 60°); the angle γ between the normal to each ring must fall between 0° and ±the γ angle cutoff (default 30°) (Fig. 1).

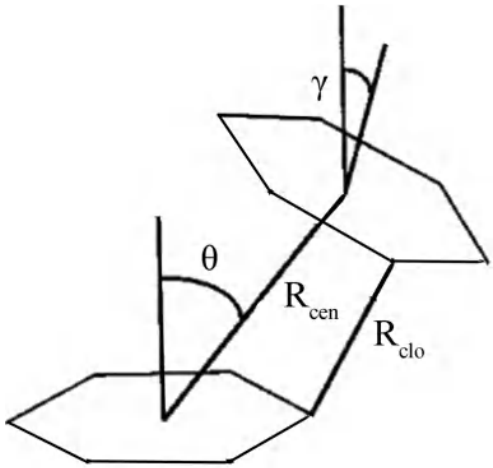

Fig. 1. The parameter for π–π stacking interaction.

3. Results and discussion

3.1. The docking of DNA and BAF2(WT):Em^{LEM}

The Gly25Glu mutation of BAF which affects DNA binding causes cellular mislocalization of emerin (Bengtsson and Wilson, 2006). So we docked two pairs of DNA with BAF2:Em^{LEM}, respectively to investigate the interaction between BAF2 and Em^{LEM}. The DNA2:BAF2(WT):Em^{LEM} ternary complex is thus formed (Fig. 2a). The X-ray crystal structure 2BZF resolved by experimenters contains just two pairs of DNA and BAF2, but without Em^{LEM}. It has been suggested that the binding of DNA and BAF is nonspecific and BAF residues interact with the backbone of DNA but not base pair (Bradley et al., 2005). On the other hand, the structure 2ODG contains Em^{LEM} and BAF2, but without DNA. However, there is not any ternary structure containing DNA, BAF2, and Em^{LEM}. Therefore, we used ZDOCK module to obtain the complex structure of DNA2:BAF2:Em^{LEM}. The reliability of the docking method has been proved in our previous work (Shang et al., 2014). The results show that Gly25Glu mutation attenuates the interaction between DNA and BAF significantly. Related experiments (Shimi et al., 2004) suggest that during the bridging of Em^{LEM} or DNA, BAF2 has no conformational changes. The result indicates that the rigid docking method (ZDOCK) is compatible for our simulating investigation. Gly25 in both chains of BAF2(WT) are mutated to Glu25 by Discovery Studio 2.5. Thus, the DNA2:BAF2 (MT):Em^{LEM} complex is constructed. BAF2 is a centrosymmetric homodimer. But Em^{LEM} is not symmetrical (Fig. 2a). It suggests that the binding sites from the two chains of BAF2 are not identical (Cai et al., 2007). The Gly25 of BAF2(WT) locates in the loop of helix–hairpin–helix (HhH) motif (Fig. 2), which is the interface between BAF and DNA. However, the mutation Glu25 in BAF2(MT) is distant from the binding site of Em^{LEM}. The remote effect of Glu25 on Em^{LEM} binding site will be further discussed.

3.2. MD simulation analysis

The conformational characteristics of DNA2:BAF2(WT):Em^{LEM} complex and DNA2:BAF2(MT):Em^{LEM} complex were investigated by MD simulation method at 300 K with explicit water. After 30 ns MD simulation, the average RMSD value of DNA2:BAF(WT):Em^{LEM} complex is 2.74 Å. The RMSD values have a small deviation from the average value. The WT complex reaches equilibrium after 5 ns simulation, which implies that the complex structure is rather stable. The value of DNA2:BAF2(MT):Em^{LEM} complex is 3.31 Å, which is higher than the former one. However, the RMSD values deviate quite largely from the average value. The trajectory fluctuations of MT complex are also more violent than that of WT complex (Fig. 3). It indicates that mutating Glu25 in BAF2 may change the conformation of MT complex in certain areas during 30 ns MD simulation.

3.3. Binding free energy between Em^{LEM} and BAF2

The binding free energies between BAF2 and Em^{LEM} are shown in Table 1. These energies determine a stable binding mode for DNA2:BAF2:Em^{LEM} complexes. The key hydrophobic residues of BAF2(WT) involving Val51, Leu52 and Leu58 from chain A (where uppercase letters indicate residues from chain A); gly38, phe39 and val51 from chain B (where lowercase letters indicate residues from chain B) interact with *Gly24, Pro25 and Val26* of Em^{LEM} (italics denote residues of Em^{LEM}). Key electrostatic residues including Asp55, Asp57, Glu61 and Asp65 of BAF2(WT) chain A, glu36 of chain B interact with *Arg17 and Lys36* of Em^{LEM}

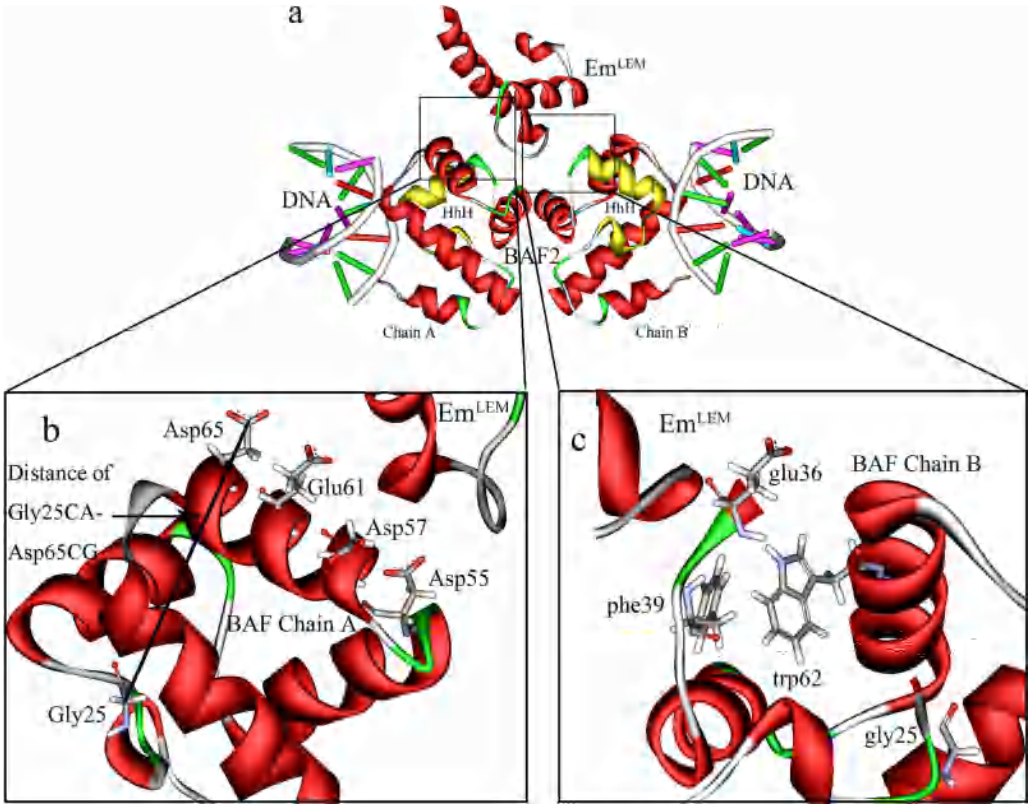

Fig. 2. (a) The docking structure of DNA2:BAF2(WT):Em^{LEM} complex. The HhH motifs are represented by yellow chains in BAF2. (b) The key residues of BAF chain A. The initial uppercase letters indicate residues from chain A. (c) The key residues of BAF chain B. The lowercase letters indicate residues from chain B. A part of the HhH motif is deleted. (For interpretation of the references to color in this figure legend, the reader is referred to the web version of this article.)

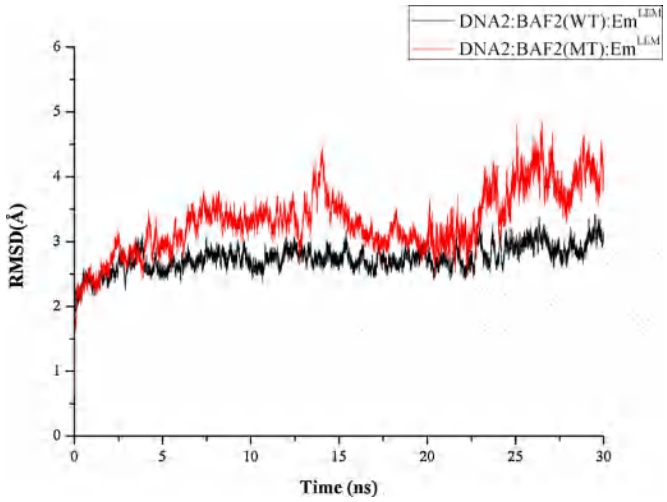

Fig. 3. The RMSD plots of DNA2:BAF2:Em^{LEM} within 30 ns simulation.

(Table 2, Fig. 2b and c). The results above are coordinated with the experimental data (Cai et al., 2007). Comparing with that of residues in BAF2(WT), the binding free energies of following residues in BAF2(MT) decrease expressively: Asp55, Asp57, Glu61 and Asp65 from chain A; glu36 and phe39 from chain B. The total binding free energy between BAF2(MT) and Em^{LEM} (-127.79 kcal mol^{-1}) is lower than that between BAF2(WT) and Em^{LEM} (-72.29 kcal mol^{-1}), which indicates that BAF2(MT) binds with Em^{LEM} more tightly. Interestingly, with the E_{ele} decreasing to -628.96 kcal mol^{-1} in BAF2(MT), E_{vdw} in that increases to -17.78 kcal mol^{-1} conversely (Table 1), which suggests that the mutation hydrophilic Glu25 may disturb the hydrophobic area of binding site between BAF2(MT) and Em^{LEM}. Table 1 shows that E_{ele} contributes greatly to the interaction between BAF2 and Em^{LEM}. But polar solvation effect (ΔG_{GB}) counteracts most of the vacuum energy from E_{ele}. Otherwise, nonpolar solvation effect (ΔG_{SASA}) and entropy ($-T\Delta S$) contribute a little to the total energy (ΔG_{tot}).

3.4. The key residues influencing the interaction between Em^{LEM} and BAF2

Gly25Glu mutation may change the distribution of charge in BAF2. The electric repulsion causes other electronegative residues such as Asp55, Asp57, Glu61 and Asp65 from chain A to form stronger electrostatic interaction with Em^{LEM} (Table 1). To evaluate the charge variation influenced by no. 25 residues, we choose CA atom of no. 25 residues (Gly25 or Glu25) and CG atom of Asp65 for instance to determine the distances (Fig. 4). 60,000 snapshots were adopted during 30 ns simulation time. The average distances are 17.33 and 21.47 Å, respectively. The results show that mutation Glu25 can convert the orientation of the same electrical residue side chain towards Em^{LEM}.

The binding free energy of glu36 from chain B decreases in BAF2 (MT) (Tables 2 and 3). The no. 25 residues and glu36 of chain B locate in HhH motif (Fig. 2a) which mainly contributes to interact with the DNA (Bradley et al., 2005). However, the results suggest that HhH motif in chain B also interacts with Em^{LEM} (Fig. 2c). The

Table 2
Interaction energies between some important BAF2 residues and Em^{LEM} in DNA2:BAF2(WT):Em^{LEM} complexes (kcal mol^{-2}).

Residue	E_{vdw}	E_{ele}	ΔG_{GB}	ΔG_{SASA}	E_{total}
A_Gly47	−0.06	−7.58	6.44	−0.01	−1.21
A_Gln48	−1.62	−14.92	12.68	−0.24	−4.10
A_Leu52	−1.22	−2.18	1.85	0.48	−1.07
A_Lys53	−2.20	−12.30	10.46	0.63	−3.41
A_Asp55	−0.27	−8.76	7.45	−0.04	−1.62
A_Asp57	−0.20	−38.50	32.73	−0.03	−6.01
A_Glu61	−0.22	−41.69	40.14	0.33	−1.44
A_Trp62	−0.25	−18.24	14.25	0.34	−3.90
A_Asp65	−1.04	−57.00	54.15	−0.16	−4.05
B_leu34	−0.38	−9.82	8.35	−0.06	−1.91
B_glu35	−0.90	−22.22	20.14	−0.14	−3.12
B_glu36	−0.01	−14.05	11.94	0.00	−2.12
B_arg37	−3.56	−27.98	31.43	−1.28	−1.39
B_gly38	−1.10	3.95	−3.36	−0.77	−1.28
B_phe39	−2.73	−2.45	2.08	−0.41	−3.51
B_asp40	−0.38	−6.57	5.58	−0.06	−1.43
B_val44	−0.92	−1.64	1.39	−0.14	−1.31
B_val51	−1.35	−2.01	1.71	−0.20	−1.85
B_trp62	−0.01	−9.78	8.31	0.00	−1.48
B_thr66	−0.51	−11.59	9.85	−0.08	−2.33
C_ Asp9	−1.62	−51.73	50.53	−0.75	−2.07
C_ Thr10	−0.02	−4.12	0.84	−0.16	−3.46
C_ Thr13	−0.09	−36.95	34.07	0.15	−2.82
C_ Arg17	0.19	−24.80	22.09	0.00	−2.52
C_ His23	−1.84	−3.01	2.97	−0.50	−2.38
C_ Gly24	−0.40	−6.42	4.24	−0.06	−2.64
C_ Pro25	2.38	−6.75	3.52	−0.38	−1.23
C_ Val26	−1.81	−1.85	0.97	−0.29	−2.98
C_ Val27	−1.40	−9.20	9.03	−0.22	−1.79
C_Ser29	−1.93	−12.17	12.26	−0.30	−2.14
C_Thr30	0.30	−10.09	8.35	−0.05	−1.49
C_Leu33	−0.30	−16.72	13.61	−0.05	−3.46
C_Lys36	0.11	−19.88	14.74	0.00	−5.03

Gly25Glu mutation may exclude the side chain of glu36 to another direction. Thus glu36 forms a stronger salt bridge with *Arg17* of Em^{LEM} (Cai et al., 2007).

Another interesting residue is Trp62 of BAF2. Further investigation reveals that Trp62 plays different roles in either chain. We adopt 60,000 snapshots during 30 ns simulation time to determine the centroid distance between two aromatic rings of trp62 and phe39 of BAF2(WT) chain B. The average distance is 5.40 Å (Fig. 5, red). The average closest atom distance is 3.77 Å (Fig. 5, black). Meanwhile, most θ and γ angles are in the acceptable angle cutoff, respectively (Fig. 6). The results above show that there is a π–π stack between trp62 and phe39 in BAF2(WT) chain B (Wang et al., 2013). The binding free energy is -3.47 kcal mol^{-1}. But the stack is destroyed in BAF2(MT) chain B (the data are not shown), which leads trp62 strengthening interaction with no. 25 residue (0.77 kcal mol^{-1} of gly25 to -4.77 kcal mol^{-1} of glu25). Meanwhile, the mutation also induces phe39 to form much stronger interaction with Em^{LEM}. The binding free energies of phe39 decrease from -3.51 kcal mol^{-1} in WT to -14.03 kcal mol^{-1} in MT towards Em^{LEM} (Table 3). The results reveal that Gly25Glu mutation is the ultimate reason for the destruction of π–π stack in BAF2(MT) chain B.

There is no π–π stack detected in either WT or MT of chain A (the data are not shown). It also partially suggests that the

Table 1
Binding free energies (kcal · mol^{-1}) and its components between BAF2 and Em^{LEM}.

System	E_{vdw}	E_{ele}	ΔG_{GB}	ΔG_{SASA}	$\Delta G_{MM\text{-}GB/SA}$[a]	$-T\Delta S$	ΔG_{tot}[b]
Wild type	-27.22 ± 0.84	-516.52 ± 3.46	463.22 ± 3.67	-2.99 ± 0.16	-83.51 ± 0.79	11.22 ± 0.21	-72.29 ± 2.37
Mutant type	-17.78 ± 0.39	-628.96 ± 5.37	503.17 ± 3.39	-1.95 ± 0.13	-145.52 ± 1.58	17.73 ± 0.15	-127.79 ± 1.59

[a] $\Delta G_{MM-GB/SA} = E_{ele} + E_{vdw} + \Delta G_{GB} + \Delta G_{SASA}$.
[b] $\Delta G_{tot} = \Delta G_{MM-GB/SA} - T\Delta S$.

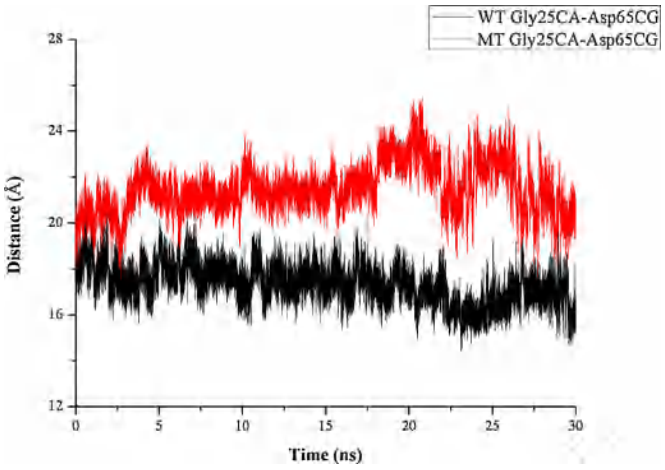

Fig. 4. The distances between CA atom of no. 25 residues and CG atom of Asp65 from BAF2 chain A during 30 ns MD simulation.

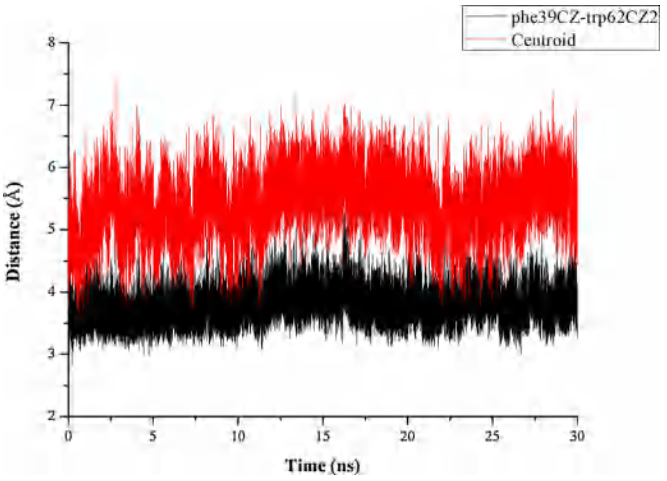

Fig. 5. Two distance data from BAF2(WT) chain B during 30 ns MD simulation. The centroid distance between benzene ring in phe39 and indole ring in trp62 (red). The distance between CZ atom in phe39 and CZ2 atom in trp62 (black). (For interpretation of the references to color in this figure legend, the reader is referred to the web version of this article.)

chemical environments of the two subunits of BAF2 are different (Cai et al., 2007). In spite of this, Trp62 is still a pivotal residue forming a stronger interaction with MT Glu25 (−7.67 kcal mol^{-1}), than that with WT Gly25 (0.03 kcal mol^{-1}). This interaction weakens the binding free energy between Trp62 and Em^{LEM} from −3.90 kcal mol^{-1} to −1.85 kcal mol^{-1} (Tables 2 and 3). Through analysis of the key residues, it is revealed that the electrostatic effect mainly contributes to strengthen the affinity to Em^{LEM} in BAF2(MT) chain A. However, in BAF2(MT) chain B, only glu36 affords electrostatic interaction with Em^{LEM}. Due to the disruption of π–π stack, phe39 participates in binding with Em^{LEM}.

Related experiment observed the interaction between BAF2 and emerin but without binding of DNA, and suggested that Gly25Glu mutant is inactive for binding to emerin in vitro, but might retain the ability to interact with BAF:DNA complexes (Haraguchi et al., 2001). The structure of BAF2 may be destroyed by the mutation. However, our molecular simulation shows that BAF2(MT) has even stronger interaction with in DNA2:BAF2:Em^{LEM} complex, which seems to be contrary to the experiment results. We suspect that the key point is the existence of DNA. 30 ns MD simulations were performed on DNA2:BAF2(WT) and BAF2(WT), DNA2:BAF2(MT) and BAF2(MT). The MD trajectory comparisons show that the fluctuations of DNA2:BAF2(WT) and dissociative BAF2(WT) are almost the same (Fig. 7). The average RMSD values are 2.00 and 2.28 Å, respectively. However, the average RMSD values of DNA2:BAF2(MT) and dissociative BAF2(MT) are 2.20 and 2.95 Å, respectively (Fig. 8). Our previous study (Shang et al., 2014) revealed that DNA can stabilize the structure of BAF(WT) or BAF(MT). When the DNA is docked to the BAF2:Em^{LEM} complex, the DNA may influence the structure variation of either BAF2(WT) or BAF2(MT). The root mean square fluctuation (RMSF) values show that the main chain of BAF2(MT) keeps slight movement with the existence of DNA. The residues Gln5-Gly31, Asp55-Asp65, glu13-lys41 of DNA2:BAF2(MT) are the three major variation groups compared with that of dissociative BAF2(MT) (Fig. 9). The RMSF values of DNA2:BAF2(WT) and BAF2(WT) are much lower than the MT structures (Fig. 10). It indicates that the main chains of DNA2:BAF2(WT) and BAF2(WT) are stable during MD simulations. The

Table 3
Interaction energies between some important BAF2 residues and Em^{LEM} in DNA2:BAF2(MT):Em^{LEM} complexes (kcal mol^{-1}).

Residue	E_{vdw}	E_{ele}	ΔG_{GB}	ΔG_{SASA}	E_{total}
A_Gln48	−0.10	−18.59	15.80	−0.02	−2.91
A_Leu50	−0.27	−7.65	6.50	−0.04	−1.46
A_Val51	−3.34	4.09	−3.48	−0.80	−3.53
A_Asp55	−0.53	−32.52	27.64	−0.08	−5.49
A_Glu56	−0.07	−24.72	21.01	−0.01	−3.79
A_Asp57	−0.36	−34.68	24.98	−0.05	−10.11
A_Leu58	−0.39	−5.09	4.33	−0.06	−1.21
A_Glu61	1.78	−65.72	51.91	0.27	−11.76
A_Trp62	−1.08	−2.08	1.77	−0.46	−1.85
A_Asp65	−2.42	−61.93	47.64	0.36	−16.35
A_Ala69	0.00	−13.49	11.47	0.00	−2.02
B_lys33	−0.16	−21.04	17.88	−0.02	−3.34
B_glu36	−2.53	−66.55	56.57	−0.38	−12.89
B_gly38	−2.01	0.20	−0.17	−0.30	−2.28
B_phe39	−0.31	−24.44	10.77	−0.05	−14.03
B_val44	−1.21	−11.69	9.94	−0.18	−3.14
B_val51	−0.88	−3.66	3.11	−0.13	−1.56
C_ Asp9	−0.35	−75.90	74.16	1.08	−1.01
C_ Arg17	−0.27	−29.19	22.38	0.00	−7.08
C_ Gly24	−0.58	−9.29	6.13	−0.08	−3.82
C_ Pro25	3.45	−9.76	5.08	−0.55	−1.78
C_ Val26	−2.62	−2.68	1.40	0.42	−3.48
C_ Val27	−2.02	−13.30	13.05	−0.31	−2.58
C_Thr30	0.44	−14.58	12.07	−0.08	−2.15
C_Leu33	−0.40	−24.16	19.67	−0.07	−4.96
C_Lys36	−0.16	−50.98	40.66	0.00	−10.48

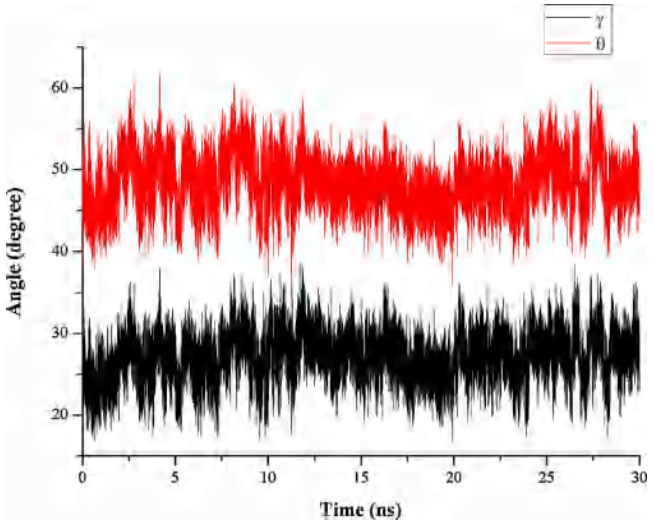

Fig. 6. The γ (black) and θ (red) angle variation between benzene ring in phe39 and indole ring in trp62 from BAF2(WT) chain B during 30 ns MD simulation.

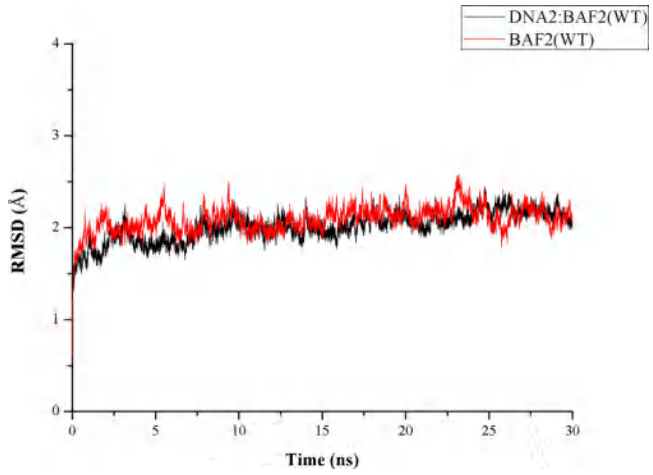

Fig. 7. The RMSD plots of DNA2:BAF2(WT) and BAF2(WT) complexes within 30 ns simulation.

results are consistent with our conclusions mentioned above. According to our simulations, Gly25Glu mutation and introduction of DNA are two contrary forces to influence the conformation change of BAF2 during MD simulation.

LEM proteins involve many activities, including nuclear assembly, DNA replication, actin dynamics, signaling downstream of the TGF-β family structural roles in nuclear assembly and chromatin architecture during the interphase (Gruenbaum et al., 2005). Besides, BAF might affect gene expression at multiple levels (Holaska et al., 2003). Gly25Glu mutation in BAF2(MT) can result in significant impact on DNA2:BAF2:Em^{LEM} interaction. But the effects on each subunit of BAF2 are distinct. The mutation Glu25 makes some key residues of BAF2(MT) convert to Em^{LEM} (Fig. 4). Related experiments (Wolff et al., 2001; Furukawa, 1999; Shimi et al., 2004; Shumaker et al., 2001) propose that Em^{LEM} binding with BAF2 is a 'touch and go' model during interphase, which reveals that the contact between Em^{LEM} and BAF2 is frequent and transient. When BAF2(MT) reinforce the interaction with Em^{LEM}, the dynamic movement between BAF2(MT) and Em^{LEM} would be disturbed. Further, the mislocalization of emerin would disorder the downstream pathways by changing the localization or stability of lamin A (Haraguchi et al., 2001). BAF, lamins and LEM proteins appear to have a special relationship. Each can directly bind the other (Holaska et al., 2003). Disruptions

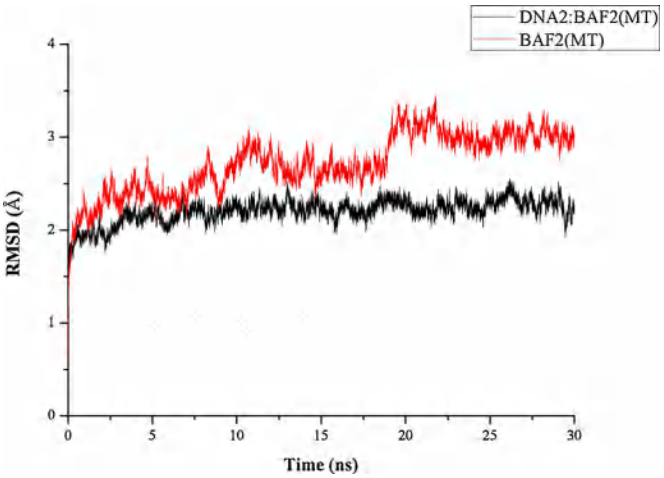

Fig. 8. The RMSD plots of DNA2:BAF2(MT) and BAF2(MT) complexes within 30 ns simulation.

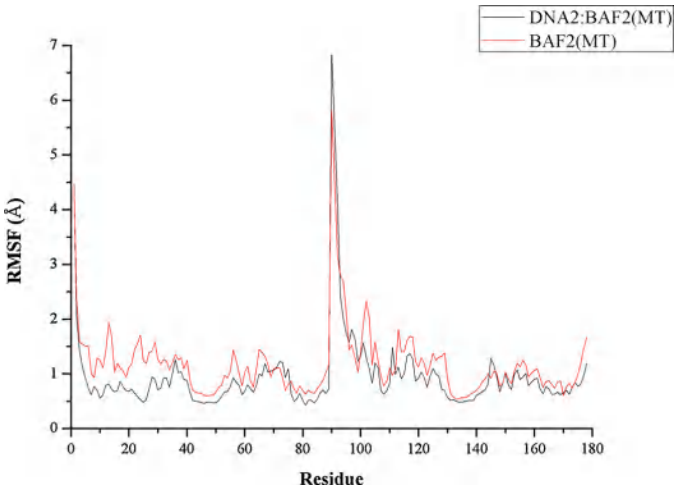

Fig. 9. The RMSF values of DNA2:BAF2(MT) and BAF2(MT) residues.

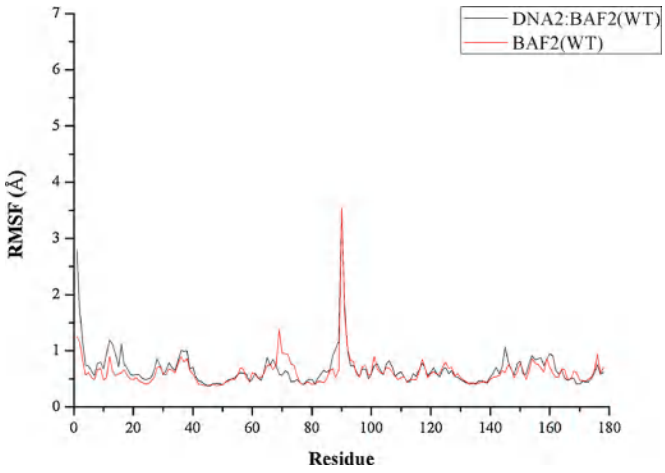

Fig. 10. The RMSF values of DNA2:BAF2(WT) and BAF2(WT) residues.

in the attachments between LEM proteins and BAF2 may also be functionally relevant for human diseases caused by defects in nuclear lamina proteins (Bonne et al., 2000; Cohen et al., 2001). Further studies are needed to understand the interactions of BAF2 with LEM proteins and lamins.

4. Conclusion

We utilize Discovery Studio 2.5/ZDOCK module and Amber11 software package to perform DNA2:BAF2(WT):Em^{LEM} and DNA2:BAF2(MT):Em^{LEM} simulations. The results show that Gly25Glu mutation can disturb the structure of DNA2:BAF2(MT):Em^{LEM} in certain areas. The RMSD fluctuation of DNA2:BAF2(MT):Em^{LEM} simulations is more violent than that of DNA2:BAF2(WT):Em^{LEM}. We calculated the binding free energies between BAF2 (WT) or (MT) and Em^{LEM}. The total energy of BAF2(WT):Em^{LEM} ($-72.29\,kcal\,mol^{-1}$) is higher than that of BAF2(MT):Em^{LEM} ($-127.79\,kcal\,mol^{-1}$). It means the interaction between BAF2 (MT) and Em^{LEM} is more stronger than BAF2(WT) and Em^{LEM}. With the E_{ele} decreasing to $-628.96\,kcal\,mol^{-1}$ in BAF2(MT), E_{vdw} increases to $-17.78\,kcal\,mol^{-1}$ in BAF2(MT). It indicates that the mutation Glu25 may disturb the hydrophobic area of binding site between BAF2(MT) and Em^{LEM}. The electrostatic interaction is

the main determinant in the BAF2 and Em^{LEM} interaction. Such as electronegative residues Asp55, Asp57, Glu61 and Asp65 from chain A, glu36 from chain B of BAF2 contribute to interact with Em^{LEM}. Besides, trp62 in chain B of BAF2 is another key residue. In BAF2(WT), trp62 can form a π–π stack ($-3.47\ kcal\ mol^{-1}$) with phe39. But π–π stack disappears in BAF2(MT). The trp62 forms an interaction ($-4.77\ kcal\ mol^{-1}$) with glu25, conversely. The phe39 converts to interact with Em^{LEM} ($-14.03\ kcal\ mol^{-1}$). There is no π–π stack detected between Trp62 and Phe39 from chain A. But Trp62 also forms a strong interaction with MT Glu25 ($-7.67\ kcal\ mol^{-1}$). And the binding free energy of Trp62 increase from $-3.90\ kcal\ mol^{-1}$ to $-1.85\ kcal\ mol^{-1}$ towards Em^{LEM}. Gly25Glu mutation can change the distribution of the charge in BAF2 to disturb the localization of Em^{LEM} on BAF2. Our simulation reveals that the introduction of DNA may change the conformation of BAF(MT). Thus, key residues of BAF(MT) convert to strengthen the interaction with Em^{LEM}. The mutation Glu25 proposed in this study is useful for understanding the potential mechanisms of BAF2 and Em^{LEM} interaction. Our results may be helpful for further experimental investigations and BAF docking studies.

Acknowledgement

This work is supported by Natural Science Foundation of China (Grant Nos. 21273095, 20903045, 21203072)

Reference

Accelrys Software Inc, 2007. Discovery Studio User Guide. Accelrys Software Inc..
Bengtsson, L., Wilson, K.L., 2006. Barrier-to-autointegration factor phosphorylation on Ser-4 regulates emerin binding to lamin A in vitro and emerin localization in vivo. Mol. Biol. Cell 17, 1154–1163.
Bonne, G., Mercuri, E., Muchir, A., et al., 2000. Clinical and molecular genetic spectrum of autosomal dominant Emery-Dreifuss muscular dystrophy due to mutations of the lamin A/C gene. Ann. Neurol. 48, 170–180.
Bradley, C.M., Ronning, D.R., Ghirlando, R., et al., 2005. Structural basis for DNA bridging by barrier-to-autointegration factor. Nat. Struct. Mol. Biol. 12, 935–936.
Cai, M., Huang, Y., Ghirlando, R., et al., 2001. Solution structure of the constant region of nuclear envelope protein LAP2 reveals two LEM-domain structures: one binds BAF and the other binds DNA. EMBO J. 20, 4399–4407.
Cai, M., Huang, Y., Suh, J.Y., et al., 2007. Solution NMR structure of the barrier-to-autointegration factor-emerin complex. J. Biol. Chem. 19, 14525–14535.
Capanni, C., Squarzoni, S., Cenni, V., et al., 2012. Familial partial lipodystrophy, mandibuloacral dysplasia and restrictive dermopathy feature barrier-to-auto-integration factor (BAF) nuclear redistribution. Cell Cycle 11, 3568–3577.
Case, D.A., Cheatham III, T.E., Darden, T., et al., 2005. The Amber biomolecular simulation programs. J. Comput. Chem. 26, 1668–1688.
Cohen, M., Lee, K.K., Wilson, K.L., et al., 2001. Transcriptional repression, apoptosis, human disease and the functional evolution of the nuclear lamina. Trends Biochem. Sci. 26, 41–47.
D'Angelo, M.A., Hetzer, M.W., 2006. The role of the nuclear envelope in cellular organization. Cell. Mol. Life Sci. 63, 316–332.
Essmann, U., Perera, L., Berkowitz, M.L., et al., 1995. A smooth particle mesh Ewald method. J. Chem. Phys. 103, 8577–8593.
Furukawa, K.J., 1999. LAP2 binding protein 1 (L2BP1/BAF) is a candidate mediator of LAP2-chromatin interaction. Cell Sci. 112, 2485–2492.
Furukawa, K., Sugiyama, S., Osouda, S., et al., 2003. Barrier-to-autointegration factor plays crucial roles in cell cycle progression and nuclear organization in Drosophila. J. Cell Sci. 116, 3811–3823.
Gohlke, H., Kiel, C., Case, D.A., 2003. Insights into protein-protein binding by binding free energy calculation and free energy decomposition for the Ras–Raf and Ras–RalGDS complexes. J. Mol. Biol. 330, 891–914.
Grosdidier, A., Zoete, V., Michielin, O., 2011. Fast docking using the CHARMM force field with EADock DSS. J. Comput. Chem. 32, 2149–2159.
Gruenbaum, Y., Margalit, A., Goldman, R.D., et al., 2005. The nuclear lamina comes of age. Nat. Rev. Mol. Cell Biol. 6, 21–31.
Haque, F., Mazzeo, D., Patel, J.T., et al., 2010. Mammalian SUN protein interaction networks at the inner nuclear membrane and their role in laminopathy disease processes. J. Biol. Chem. 285, 3487–3498.
Haraguchi, T., Koujin, T., Segura-Totten, M., et al., 2001. BAF is required for emerin assembly into the reforming nuclear envelope. J. Cell Sci. 114, 4575–4585.
Holaska, J.M., 2008. Emerin and the nuclear lamina in muscle and cardiac disease. Circ. Res. 103, 16–23.
Holaska, J.M., Lee, K.K., Kowalski, A.K., et al., 2003. Transcriptional repressor germ cell-less (GCL) and barrier to autointegration factor (BAF) compete for binding to emerin in vitro. J. Biol. Chem. 278, 6969–6975.
Hou, T.J., Zhang, W., Case, D.A., Wang, W., 2008. Characterization of domain–peptide interaction interface: A case study on the amphiphysin-1 SH3 domain. J. Mol. Biol. 376, 1201–1214.
Huber, M.D., Guan, T., Gerace, L., 2009. Overlapping functions of nuclear envelope proteins NET25 (Lem2) and emerin in regulation of extracellular signal-regulated kinase signaling in myoblast differentiation. Mol. Cell Biol. 29, 5718–5728.
Humphrey, W., Dalke, A., Schulten, K., 1996. VMD: visual molecular dynamics. J. Mol. Graph. 14, 33–38.
Jorgensen, W.L., Chandraskhar, J., Madura, J., et al., 1983. Comparison of simple potential functions for simulating liquid water. J. Chem. Phys. 79, 926–935.
Lee, M.S., Craigie, R., 1998. A previously unidentified host protein protects retroviral DNA from autointegration. Proc. Natl. Acad. Sci. 95, 1528–1533.
Liang, W.C., Mitsuhashi, H., Keduka, E., et al., 2011. TMEM43 mutations in emery-dreifuss muscular dystrophy-related myopathy. Ann. Neurol. 69, 1005–1013.
Lin, F., Blake, D.L., Callebaut, L., et al., 2000. MAN1, an inner nuclear membrane protein that shares the LEM domain with lamina-associated polypeptide 2 and emerin. J. Biol. Chem. 275, 4840–4847.
Markiewicz, E., Tilgner, K., Barker, N., et al., 2006. The inner nuclear membrane protein emerin regulates beta-catenin activity by restricting its accumulation in the nucleus. EMBO J. 25, 3275–3285.
McGaughey, G.B., Gagné, M., Rappé, A.K., 1998. Pi-stacking interactions: alive and well in proteins. J. Biol. Chem. 273, 15458–15463.
Muchir, A., Pavlidis, P., Bonne, G., et al., 2007. Activation of MAPK in hearts of EMD null mice: similarities between mouse models of X-linked and autosomal dominant Emery Dreifuss muscular dystrophy. Hum. Mol. Genet. 16, 1884–1895.
Muchir, A., Pavlidis, P., Decostre, V., et al., 2007. Activation of MAPK pathways links LMNA mutations to cardiomyopathy in Emery-Dreifuss muscular dystrophy. J. Clin. Invest. 117, 1282–1293.
Muchir, A., Shan, J., Bonne, G., et al., 2009. Inhibition of extracellular signal-regulated kinase signaling to prevent cardiomyopathy caused by mutation in the gene encoding A-type lamins. Hum. Mol. Genet. 18, 241–247.
Ode, H., Matsuyama, S., Hata, M., et al., 2007. Mechanism of drug resistance due to N88S in CRF01_AE HIV-1 protease, analyzed by molecular dynamics simulations. J. Med. Chem. 50, 1768–1777.
Segura-Totten, M., Wilson, K.L., 2004. BAF: roles in chromatin, nuclear structure and retrovirus integration. Trends Cell Biol. 14, 261–266.
Segura-Totten, M., Kowalski, A.K., Craigie, R., et al., 2002. Barrier-to-autointegration factor: major roles in chromatin decondensation and nuclear assembly. J. Cell. Biol. 158, 475–485.
Shang, Y.D., Zhang, J.L., Zheng, Q.C., et al., 2014. Molecular simulation investigation on the interaction between barrier-to-autointegration factor or its Gly25Glu mutant and DNA. J. Mol. Model. 20, 2246–2254.
Shimi, T., Koujin, T., Segura-Totten, M., et al., 2004. Dynamic interaction between BAF and emerin revealed by FRAP, FLIP, and FRET analyses in living HeLa cells. J. Struct. Biol. 147, 31–41.
Shumaker, D.K., Lee, K.K., Tanhehco, Y.C., et al., 2001. LAP2 binds to BAF center dot DNA complexes: requirement for the LEM domain and modulation by variable regions. EMBO J. 20, 1754–1764.
Swanson, J.M., Henchman, R.H., McCammon, J.A., 2004. Revisiting free energy calculations: a theoretical connection to MM/PBSA and direct calculation of the association free energy. Biophys. J. 86, 67–74.
Tilgner, K., Wojciechowicz, K., Jahoda, C., et al., 2009. Dynamic complexes of A-type lamins and emerin influence adipogenic capacity of the cell via nucleocyto-plasmic distribution of beta-catenin. J. Cell Sci. 122, 401–413.
Wang, Y., Zheng, Q.C., Zhang, J.L., 2013. Highlighting a π– interaction: a protein modeling and molecular dynamics simulation study on Anopheles gambiae glutathione S-transferase 1–2. J. Mol. Model. 19, 5213–5223.
Wen, X.X., Nan, S.B., Huang, Y., 2012. Studies of interaction between GABA and mutant GABAaR. Chem. J. Chinese. Univ. 33, 2708–2715.
Wheeler, Ellis, J.A., 2010. Molecular signatures of Emery-Dreifuss muscular dystrophy. Biochem. Soc. Trans. 36, 1354–1358.
Wiehe, K., Pierce, B., Mintseris, J., et al., 2005. ZDOCK and RDOCK performance in CAPRI rounds 3, 4, and 5. Proteins 60, 207–213.
Williams, D.C., Cai, M., Clore, G.M., 2004. Molecular basis for synergistic transcriptional activation by Oct1 and Sox2 revealed from the solution structure of the 42-kDa Oct1. Sox2. Hoxb1-DNA ternary transcription factor complex. J. Biol. Chem. 279, 1449–1457.
Wolff, N., Gilquin, B., Courchay, K., et al., 2001. Structural analysis of emerin, an inner nuclear membrane protein mutated in X-linked Emery–Dreifuss muscular dystrophy. FEBS Lett. 501, 171–176.
Zhang, Q., Ragnauth, C.D., Skepper, J.N., et al., 2005. Nesprin-2 is a multi-isomeric protein that binds lamin and emerin at the nuclear envelope and forms a subcellular network in skeletal muscle. J. Cell Sci. 118, 673–687.